JOURNAL OF SOLID STATE CHEMISTRY 61, 293–300 (1986)

Morphology and Twinning Study of the Ordered Q_1 Form in $LiFeO_2$ Ferrite

R. FAMERY, P. BASSOUL, AND F. QUEYROUX

Laboratoire de Chimie du Solide Minéral, UA 450, ESPCI—10 rue Vauquelin, 75231 Paris Cedex 05, France

Received June 26, 1985

The ordered Q_1 form of $LiFeO_2$ was studied by X-ray diffraction and transmission electron microscopy. It can be deduced that the various orientation variants are associated by threes or by twos and develop some wide habit planes $\{102\}_{Q_1}$. We have specified the orientations of these planes with respect to the orientation of the disordered C_1 form $\{110\}_{C_1}$ planes. The highest number of orientation variants which would be present is equal to 27. Among them, 15 variants exhibit the first association type and the 12 other variants, the second association type.

Introduction

An order–disorder transition occurs at 670°C in lithium ferrite $LiFeO_2$: the disordered C_1 form is cubic with a NaCl-type structure (*1*); the ordered Q_1 form is tetragonal (*2*). During the $C_1 \rightarrow Q_1$ transition, an intermediate metastable Q_2 phase is formed (*3–5*).

Recently we have published a complete Q_2 phase study in this journal (*6*).

In this paper, the results related to a twinning study of the ordered Q_1 form are provided.

Preparation of the Samples—Experimental Techniques

Single crystals of the C_1 form were grown by the flux method (*7*). The crystal shape is dendritic with the main directions of growth along $\langle 100 \rangle_{C_1}$.

The ordered Q_1 form can be obtained by heating the crystals of the disordered C_1 form at temperatures between 480 and 560°C for several days. Through this process, a complete crystal transformation from the C_1 form to the Q_1 form can be achieved.

The Q_1 form has been studied by single-crystal X-ray diffraction with a Weissenberg camera (ϕ = 57.3 mm) and by transmission electron microscopy with a Jeol 100 CX microscope. Observations have been performed on fragments obtained by crushing the single crystals.

Results and Discussion

The Q_1 form is derived from the C_1 form by Fe^{3+} and Li^+ cation ordering which induces a symmetry decrease. The resulting structure symmetry is tetragonal with space group $I4_1/amd$. The unit cell parameters are

$$a_{Q_1} = b_{Q_1} = 4.045 \text{ Å}$$
$$c_{Q_1} = 8.75 \text{ Å}$$

0022-4596/86 $3.00

with: $a_{Q_1} \simeq a_{C_1}$ and $c_{Q_1} \simeq 2c_{C_1}$ ($a_{C_1} = 4.157$ Å).

The parameters of the pseudo-cubic tetragonal unit cell which is characteristic of the anion sublattice deformation are

$$a'_{Q_1} = a_{Q_1} = 4.045 \text{ Å}$$
$$c'_{Q_1} = \tfrac{1}{2}c_{Q_1} = 4.375 \text{ Å}.$$

The use of this cell permits indexing of only the fundamental lines.

The point groups are respectively $m\bar{3}m$ for the C_1 form and $4/mmm$ for the Q_1 form. One can expect a three-twinning process if the directions of the common symmetry elements between these point groups do not change during the Q_1 formation. The variant number becomes greater than three if the directions are not preserved.

In the first case, the axes related to the three variants which would be present are parallel to the C_1 unit cell axes. With the arbitrary choice we made, the 1, 2, and 3 variant axes have the following dispositions:

$$Ox_1 \| Oy_2 \| Oz_3 \| Ox_{C_1}$$
$$Oy_1 \| Oz_2 \| Ox_3 \| Oy_{C_1}$$
$$Oz_1 \| Ox_2 \| Oy_3 \| Oz_{C_1}.$$

Under these conditions, it is easy to predict the distribution of the diffraction reflections related to the three variants. The disposition of a few of the diffraction reflections is shown schematically in Fig. 1. The α angle between the $[012]_1^*$ and $[102]_2^*$ directions or $[10\bar{2}]_2^*$ and $[0\bar{1}2]_1^*$ directions is expressed by

$$\alpha = \operatorname{arctg} \frac{2a_2^*}{c_2^*} - \operatorname{arctg} \frac{c_1^*}{2b_1^*}.$$

That is

$$\alpha = 4.5°.$$

All the crystals studied by X-ray diffraction were oriented along one of the preferred lengthening directions.

The X-ray patterns so obtained exhibit various complexities. We first considered the simplest single-crystal patterns. To interpret these patterns the experimental configuration of the diffraction reflections were compared to the configuration anticipated under the assumption of three-twinning.

The rotation-crystal photographs showed that the oriented axis of these crystals corresponds to the $\langle 100 \rangle_{Q_1}$ direction. This means that the variant having the $[001]_{Q_1}$ axis parallel to this direction, the 3-variant, for example, is absent.

The Weissenberg photographs showed the presence of variants in addition to the 1 and 2 variants. Indeed, next to each reflection related to the 1 and 2 variants, one can observe some other reflections. These and the reflection they surround are characterized by the same θ angle and are con-

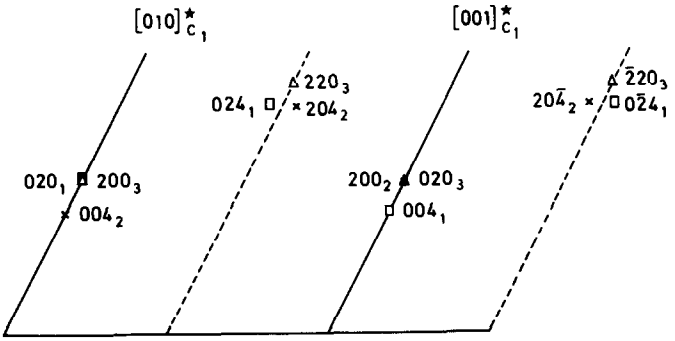

FIG. 1. Schematic configuration of the Q_1 reflections related to the 020, 022, and 002 reflections of C_1. The tetragonal deformation is strongly magnified. □. 1 variant; ×, 2 variant; △, 3 variant.

nected by diffuse streaks parallel to the origin (Fig. 2). A careful examination of these reflections permits them to be distributed systematically in two coexisting systems.

First System of Reflections

It is possible to associate two additional diffraction reflections with each reflection of 1 (or 2) variant. These reflections are situated symmetrically around the 1 (or 2) variant reflection, at a measured distance of 2.25 ± 0.05 mm. The occurrence of these additional reflections establishes four other variants denoted 1′, 1″, 2′, and 2″, in addition to the 1 and 2 variants. The comparison of the reflections having the same θ angle shows that their intensities are different. It seems reasonable to attribute these differences to an unequal development of the six variants on one hand and to the absorption process on the other hand. On the pattern shown in Fig. 2, one can only distinguish the more intense reflections. The 1′ and 1″ variants are derived from the 1 variant by a β rotation around the $[100]_1$ direction. The β angle is, respectively, equal to $4.50 \pm 0.1°$ and $-4.50 \pm 0.1°$. This value is very close to the α value previously defined. In the same manner, the 2′ and 2″ variants are derived from the 2 variant, the rotation being around the $[0\bar{1}0]_2$ direction. Consequently the $02\bar{4}_1$, $0\bar{2}4_1$, $20\bar{4}_2$ and $2\bar{0}4_2$ reflections are superimposed respectively on the $20\bar{4}_{2''}$, $2\bar{0}4_{2'}$, $02\bar{4}_{1'}$, and $0\bar{2}4_{1''}$ reflections (Fig. 3). This means that in the direct space the $(01\bar{2})_1$, $(0\bar{1}2)_1$, $(10\bar{2})_2$, and $(\bar{1}02)_2$ planes have, respectively, the same orientations as the $(10\bar{2})_{2''}$, $(\bar{1}02)_{2'}$, $(01\bar{2})_{1'}$, and $(0\bar{1}2)_{1''}$ planes.

These remarks suggest that the six characterized variants are associated three by three and are located as shown in Fig. 4. In

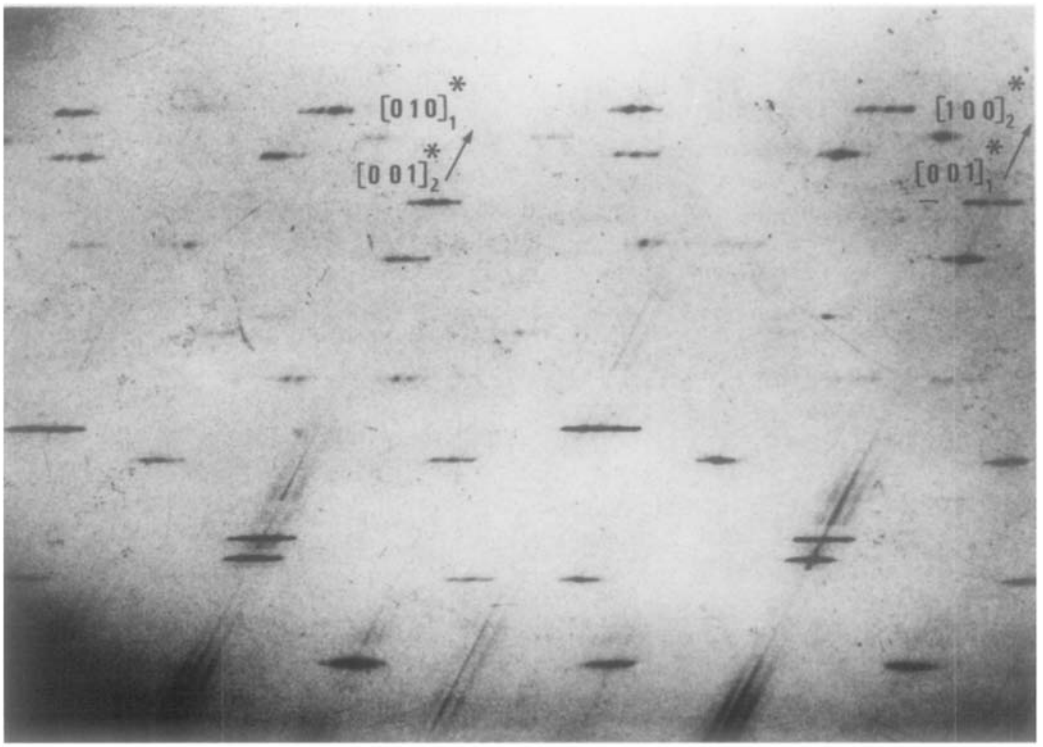

FIG. 2. Zero-level Weissenberg photograph. $\lambda K_\alpha Cu$, $\langle 100 \rangle_{Q_1}$ rotation axis.

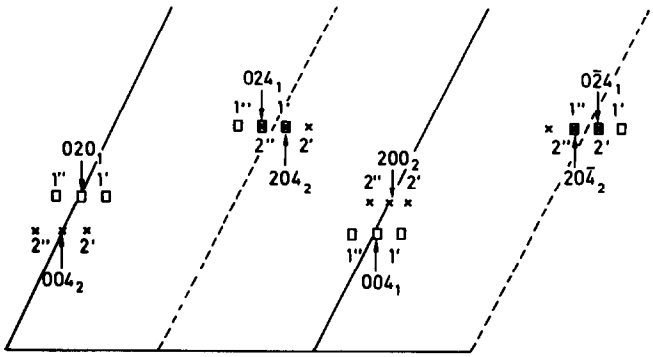

FIG. 3. First system of reflections. Schematic disposition of the 200_{Q_1}, 004_{Q_1}, 204_{Q_1} reflection types related to the: 1, 1′, 1″ variants (□) and 2, 2′, 2″ variants (×). The tetragonal deformation is strongly magnified.

these conditions, the anion sublattice of the 1 variant exhibits an invariant $\{102\}_{Q_1}$ plane with each of the anion sublattices of the 2′ and 2″ variants. The same conclusion is valid for the 2, 1′, and 1″ variants. The 1 variant develops with the 2′ and 2″ variants habit planes, the angle of which is equal to

$$2 \operatorname{arctg} \frac{2b_1}{c_1} = 85.5°.$$

The 2 variant develops with the 1′ and 1″ variants habit planes, the angle of which is equal to

$$2 \operatorname{arctg} \frac{c_2}{2a_2} = 94.5°.$$

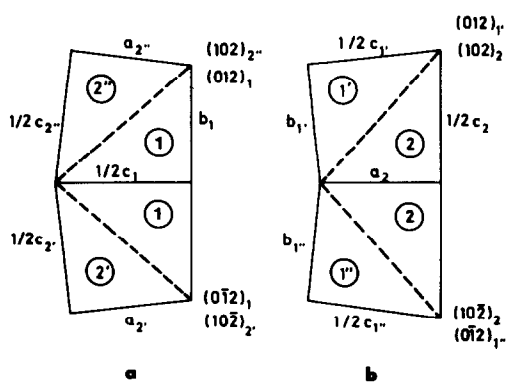

FIG. 4. 2′–1–2″ (a) and 1′–2–1″ (b) variant associations. The dashed lines indicate the habit plane traces.

Transmission electron microscopy observations confirm this interpretation as will be shown further.

To simplify this paper the set of the two associations just described will be denoted as arrangement A. These two associations are similar to the ones observed by Yamamoto *et al.* in the ferroelastic compound $Gd_2(MoO_4)_3$ (*8*).

As the Q_1 formation is associated with a symmetry decrease, one can expect to observe the two other arrangements B and C (Table I). They are derived from arrangement A by the point symmetry operators which relate the Q_1 point group $4/mmm$ to the C_1 point group $m\bar{3}m$. To avoid mistakes it is necessary to take into account the letter indexing of the variant number shown in Table I. For example, $1'_A$ and $1'_B$ characterize two different variants related, respectively, to the 1 variant by a β rotation around $[100]_1$ and $[010]_1$ directions.

TABLE I

FEATURES OF THE A, B, AND C ARRANGEMENTS

Arrangements	Associations	Common direction to the associations
A	$2'_A$–1–$2''_A$ and $1'_A$–2–$1''_A$	$[100]_1 = [010]_2$
B	$3'_B$–1–$3''_B$ and $1'_B$–3–$1''_B$	$[100]_3 = [010]_1$
C	$3'_C$–2–$3''_C$ and $2'_C$–3–$2''_C$	$[100]_2 = [010]_3$

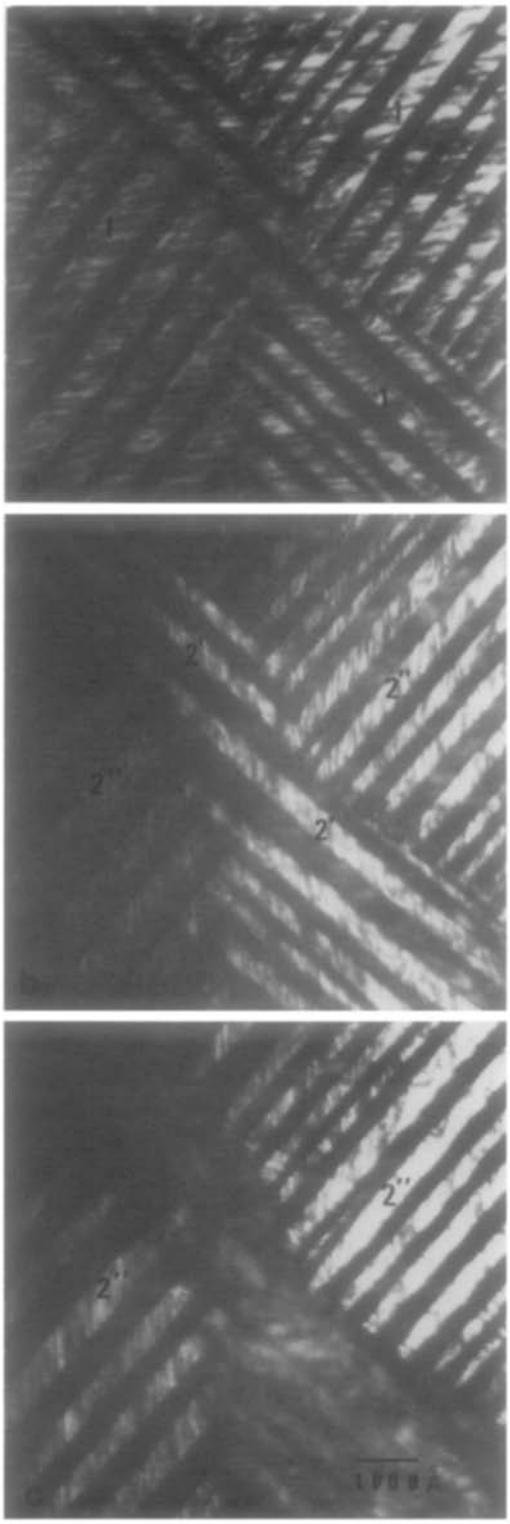

Within the various crystals studied by X-ray diffraction, examination of the pattern shows either the occurrence of any one of the arrangements or, more frequently, the occurrence of the three arrangements. So, it is easy to explain the varying complexities of the diffraction patterns obtained with the crystal studied.

The dark-field images performed by transmission electron microscopy and shown in Fig. 5 illustrate these results for the 2′-1-2″ association. These dark-field images were performed by selecting successively the 011_1 (Fig. 5a), $10\bar{5}_{2'}$ and $10\bar{5}_{2''}$ (Fig. 5b), $10\bar{5}_{2''}$ (Fig. 5c) reflections. The domains in contrast on each image correspond respectively to the 1, 2′ and 2″, 2″ variants. Their dispositions are schematically indicated in Fig. 6. The 1 variant exhibits a wide habit plane, with the 2′ and 2″ variants along $(0\bar{1}2)_1$ and $(012]_1$ planes, respectively. This is in good agreement with the expected deductions from the X-ray patterns.

A simple verification of these results consists in a measurement of the angle between the habit plane traces of the 1-2′ variants and the 1-2″ variants. This angle value, equal to 86 ± 1°, is in good agreement with the theoretical one (85.5°).

By contrast, the habit planes of the 2′ and 2″ variants are very limited because of the great range of orientations of these variants (≃9°).

The domains corresponding to the 2″ variant more frequently terminate in a point in order to minimize the contacts with the 2′ variant. From a deformation calculation, Torres *et al.* have explained this particular shape of the domains (*9, 10*).

Second System of Reflections

The Weissenberg photograph (Fig. 2) shows a second reflection system in addi-

FIG. 5. Dark-field images performed with the reflections. (a) 011_1; (b) $10\bar{5}_{2'}$ and $10\bar{5}_{2''}$; (c) $10\bar{5}_{2''}$. Observation plane: $(100)_1$.

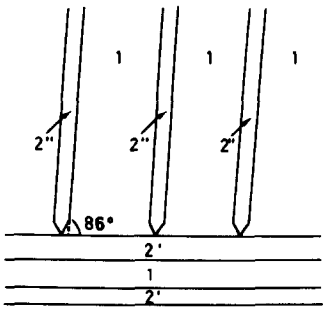

FIG. 6. Schematic representation of the variant disposition in the 2'–1–2" association.

tion to those just described. These reflections are located on each side of the reflections related to the 1 and 2 variants, at half the distance between them and the reflections related to the 1', 1", 2', and 2" variants (Fig. 7).

The presence of these reflections indicate the occurrence of other four variants denoted I', I", II', and II", in addition to those previously defined.

The I' and I" variants are derived from the 1 variant by the $\pm \beta/2$ rotations around the $[100]_1$ direction.

The II' and II" variants are derived from the 2 variant by the same rotations around the $[010]_2$ direction. From the selected conventions, one can see in Fig. 8 that the $[012]^*_{I'}$ and $[102]^*_{II''}$ directions on one hand, and the $[0\bar{1}2]^*_{II''}$ and $[10\bar{2}]_{II'}$ on the other hand are, respectively, superimposed on the $[011]^*_{C_1}$ and $[0\bar{1}1]^*_{C_1}$ directions.

These observations lead to the prediction that the habit plane between the I' and II" (or I" and II') variants is an invariant $\{102\}_{Q_1}$ plane strictly parallel to a $\{110\}_{C_1}$ plane, contrary to the observations related to the variants giving rise to the first reflection system. This disposition and the one observed in the tetragonal families of the Q_2 form (6) are the same.

The I'-II" and I"-II' associations form the arrangement denoted as A'.

As the Q_1 formation is associated with a symmetry decrease, one has to anticipate the occurrence of other two arrangements B' and C', for the reasons previously described. The A', B', and C' arrangements are indicated in Table II. For crystals with the diffraction patterns showing a greater complexity, these three arrangements coexist with those described in the preceding paragraph.

This second association type whose occurrence was deduced from an examination of the second reflection system, was corroborated by transmission electron microscopy observations.

The images shown (Fig. 9) exhibit the presence of two among the six associations just described. The observed diffraction plane has an average orientation $(1\bar{1}2)^*_{C_1}$.

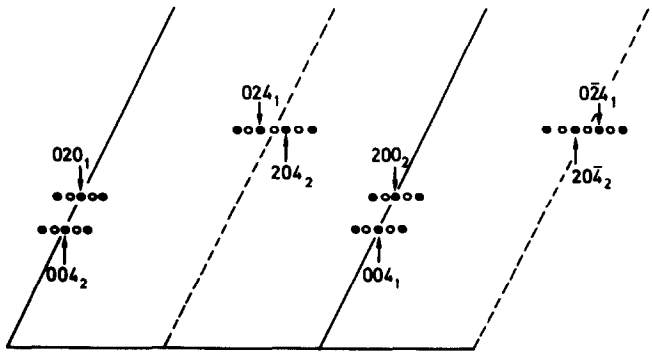

FIG. 7. Schematic disposition of the 200_{Q_1}, 004_{Q_1}, 204_{Q_1} reflection types related to the two systems of reflection: 1 system (●); 2 system (○).

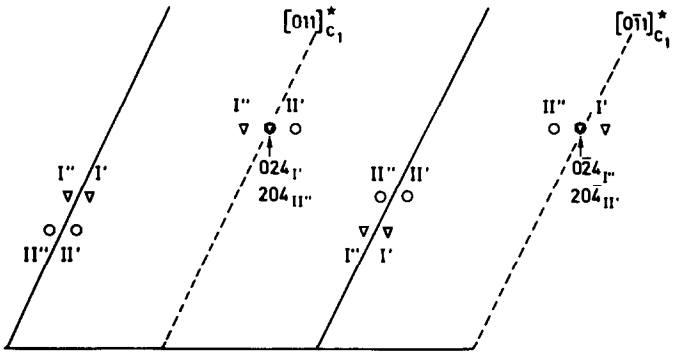

FIG. 8. Second system of reflections. Schematic disposition of the 200_{Q_1}, 004_{Q_1}, 204_{Q_1} reflection types related to the I', I" variants (▽) and II', II" variants (○). The tetragonal deformation is strongly magnified.

To identify the different domains revealed in the bright-field image (Fig. 9a) we have (1) obtained a dark-field image (Fig. 9b) by selecting simultaneously the superstructure $011_{I'_{A'}}$ and $011_{I'_{B'}}$ reflections (it is not possible to select only one reflection in the diaphram because of the shortness between these reflections); (2) obtained other two dark-field images by selecting one after another two superstructure reflections related to the $III''_{B'}$ variant and to the $II''_{A'}$ variant. In this case, the orientation of the observation plane is $(001)_{C_1}$.

The occurrence of a wide habit plane is noted between the $I'_{B'}$ and $III''_{B'}$ variants on one hand, the $I'_{A'}$ and $II''_{A'}$ variants on the other hand. The indices of these planes are respectively $(\bar{1}01)_{C_1}$ and $(011)_{C_1}$, as previously predicted. To index these planes, the angle formed by their intersections with the observed plane $(1\bar{1}2)_{C_1}$ has been measured. The value $117 \pm 0.5°$ is in good agreement with the theoretical value of 117.03°. The $I'_{B'}$ and $III''_{B'}$ variants both develop limited contacts with the $I'_{A'}$ and $II''_{A'}$ variants respectively. In addition, in the bright-field image (Fig. 9a) one can observe defects which form a curving line in the contact area of these four variants. These observations are related to the mismatch of the $I'_{B'}$ and $I'_{A'}$ anion sublattices on one hand and the $III''_{B'}$ and $II''_{A'}$ anion sublattices on the other hand.

Whatever the association type observed (Figs. 5 and 9a) the contrast is never uniform inside the variant domains. This particular feature is related to the presence of defects. It was impossible to provide an interpretation of these defects because of their great density.

Stated differently, our results show that the diffuse streaks in the X-ray diffraction patterns (see the first part of this paper) are related to fluctuations in the variant orientations. For crystals characterized by the occurrence of variants with the same $\langle 100 \rangle_{C_1}$ direction, the rotation-crystal pattern indicates that these fluctuations are a disorientation in the plane perpendicular to the $\langle 100 \rangle_{C_1}$ direction.

TABLE II

FEATURES OF THE A', B', AND C' ARRANGEMENTS

Arrangements	Associations	Habit planes	Common directions to the associations
A'	$I'_{A'}$–$II''_{A'}$	$(011)_{C_1}$	$[100]_{C_1}$
	$I''_{A'}$–$II'_{A'}$	$(0\bar{1}1)_{C_1}$	
B'	$III''_{B'}$–$I'_{B'}$	$(101)_{C_1}$	$[010]_{C_1}$
	$III'_{B'}$–$I''_{B'}$	$(\bar{1}01)_{C_1}$	
C'	$II'_{C'}$–$III''_{C'}$	$(110)_{C_1}$	$[001]_{C_1}$
	$II''_{C'}$–$III'_{C'}$	$(\bar{1}10)_{C_1}$	

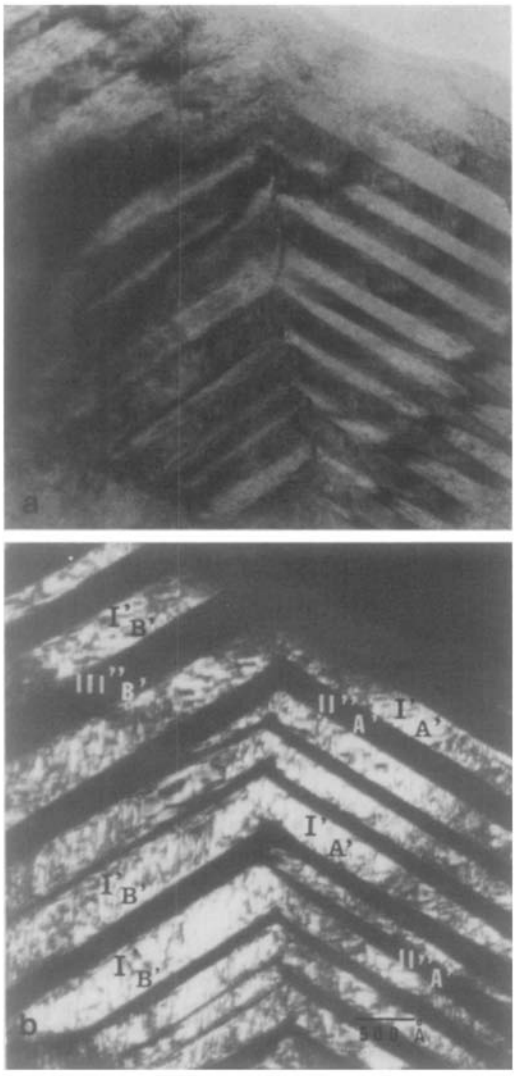

FIG. 9. Bright-field image (a) and dark-field image (b) exhibiting the two variant associations $I'_{B'}$–$III''_{B'}$ and $I'_{A'}$–$II''_{A'}$. Observation plane: $(1\bar{1}2)_{C_1}$.

These disorientations are probably related to the numerous areas where the various coherent association types are connected.

Conclusions

The X-ray diffraction and transmission electron microscopy study has allowed us to interpret the twinning of the ordered Q_1 form of $LiFeO_2$.

We have shown that inside the crystals, the various variants are associated by threes or by twos and develop some coherent $\{102\}_{Q_1}$ habit planes. The orientations of these planes are either slightly different from or else, strictly parallel to, the $\{110\}_{C_1}$ planes, according as we consider the first or the second association type.

The highest number of orientation variants which would be present is equal to 27. Among them 15 variants exhibit the first association type and the 12 other variants exhibit the second association type.

Whatever the temperature and the heating time of the Q_1 form preparation, the two association types are present in the samples; this means that their energies may be very close.

References

1. E. POSNJAK AND T. BARTH, *Phys. Rev.* **38,** 2234 (1931).
2. F. BARBLAN, E. BRANDENBERGER, AND P. NIGGLI, *Helv. Chim. Acta* **27,** 88 (1944).
3. R. COLLONGUES, *C.R. Acad. Sci.* **241,** 1577 (1955).
4. M. FAYARD, *Ann. Chim. (Paris)* **6,** 1279 (1961).
5. M. BRUNEL AND F. DE BERGEVIN, *J. Phys. Chem. Solids* **29,** 163 (1968).
6. R. FAMERY, P. BASSOUL, AND F. QUEYROUX, *J. Solid State Chem.* **57,** 178 (1985).
7. J. C. ANDERSON AND M. SCHIEBER, *J. Phys. Chem.* **67,** 1838 (1963).
8. N. YAMAMOTO, K. YAGI AND G. HONJO, *Phys. Status Solidi A* **42,** 257 (1977).
9. J. TORRES, C. ROUCAU, AND R. AYROLLES, *Phys. Status Solidi A* **70,** 659 (1982).
10. J. TORRES, C. ROUCAU, AND R. AYROLLES, *Phys. Status Solidi A* **71,** 193 (1982).